

This is a postprint version of the following published document:

Stefanovic, C., Panic, S. R., Bhatia, V., Kumar, N. & Sharma, S. (25-28 april 2021). On Higher-Order Statistics of the Channel Model for UAV-to-Ground Communications. *2021 IEEE 93rd Vehicular Technology Conference (VTC2021-Spring)*. Helsinki, Finland.

DOI: [10.1109/vtc2021-spring51267.2021.9448754](https://doi.org/10.1109/vtc2021-spring51267.2021.9448754)

On Higher-Order Statistics of the Channel Model for UAV-to-Ground Communications

Caslav Stefanovic*, Stefan R. Panic†, Vimal Bhatia‡, Nagendra Kumar§ and Sanjeev Sharma¶

*Universidad Carlos III de Madrid, Department of Signal Theory and Communications,
28911 Leganés, Spain

Email: caslav.stefanovic@uc3m.es

†Faculty of Science and Mathematics, University of Pristina, Serbia,
Email: stefan.panic@pr.ac.rs

‡Indian Institute of Technology, Indore, India, 453552
Email: vbhatia@iiti.ac.in

§National Institute of Technology Jamshedpur, Jharkhand, India, RIT Jamshedpur 831014
Email: nagendrakumar.ece@nitjsr.ac.in

¶Indian Institute of Technology (BHU), Varanasi, India, Uttar Pradesh 221005
Email: sanjeev.ece@itbhu.ac.in

Abstract—Unmanned-aerial-vehicles (UAVs) based communications are envisioned to play an important role in 5G and beyond 5G (B5G) systems. UAV-to-ground communications in urban cities are often characterized by highly dynamic propagation environments that can be described by composite fading channels. Most of the UAV-to-ground systems are based on first order (FO) performance evaluation, however the models based on FO statistics are insufficient for characterization of time variant fading channels. We provide comprehensive mathematical framework for the second order (SO) statistics over double-scattered, double-shadowed (DS-DS) fading channels, modeled as the product of double Nakagami-m (DN) and double inverse Gamma (DIG) random processes (RPs). In particular, we obtained exact mathematical expressions for average fade duration (AFD) and level crossing rate (LCR) of the proposed UAV-to-ground channel model. Moreover, the exact, integral form SO statistical expressions are approximated by Laplace Integration (LI) and exponential LI in order to provide closed form, easily computing mathematical expressions. Numerical results show that approximate and exact results are fitting well, especially for higher output threshold values. The impact of DS-DS fading severities on the SO statistics are well investigated. Furthermore, the proposed method is extended to analyze SO performances for the selection scenario of UAV with the highest signal level from among N-UAVs links.

Index Terms—B5G communications, 6G communications, Average fade duration, Level crossing rate, Unmanned aerial vehicle (UAV).

I. INTRODUCTION

In the recent years, we have seen increased research interest in unmanned aerial vehicles (UAV) based communications. UAVs are being used for parcel, medicine delivery, monitoring of social distancing, monitoring fleet, farming and others. Yet, there are many challenges needed to be addressed and among the most important is accurate channel modeling for UAV communications [1]-[2]. The urban topology is dense with buildings, features, and has huge densely populated areas. In such scenarios channel modeling and coverage due to building and structures is a major problem. UAV-to-ground

communication mainly operates in line of sight (LOS) environments with increased mobility (IM) of communication nodes. In urban cities, besides LOS-IM communications, non-LOS IM communications is expected. The UAV-to-ground channel model capable of accounting for multipath and shadowing effects, and that is in accordance with experiments can be modeled as the double-scattered, double-shadowed (DS-DS) fading channel [3]-[4]. The paper [3] provides probability density function (PDF), cumulative distribution function (CDF), outage probability and channel capacity (C) of DS-DS fading channel modeled as the products of double Nakagami-m (DN) and double inverse Gamma (DIG) random processes (RPs). However, performance analysis of UAV communications obtained in [3]-[9] are mainly observed through first order (FO) statistical measures.

In addition to evaluation of the FO statistics, level crossing rate (LCR) and average fade duration (AFD), also known as the second order (SO) statistics can further broaden understanding of the time-variant fading channels (TVFC). Namely, the LCR addresses TVFC by determining time rate of change of the signal envelope, while AFD addresses TVFC by determining the mean time of the signal envelope being below a specified threshold. In particular, those measures can be useful for the channel coding, block interleave and overall system design. Furthermore, 5G and beyond 5G (B5G) expected requirements include ultra-reliable, low-latency communications (URLLCs) which requires the system performance analysis with respect to time [10].

UAV communication performances obtained in [11]-[15] are mainly observed through SO statistical measures. However, SO performances of DS-DS UAV fading channels have not been observed in open literature so far.

This paper provides the development of a non-GBSM framework for derivation of SO statistics. The main contributions of our study are:

- Derivation of mathematical expressions for LCR and

AFD of DS-DS fading channel, modeled as the product of independent but not identically distributed (i.n.i.d) DN and DIG RPs.

- Derivation of approximate closed-form SO statistics by using Laplace integration (LI) and exponential LI.
- Confirmation of obtained SO statistical results by Monte Carlo simulations.
- SO performance analysis for the selection scenario of UAV with the highest signal level from among N-UAV links.
- Analysis of the impact of DS-DS multipath and shadowing severity parameters on the observed performance measures.

II. SYSTEM MODEL

The composite fading channel for UAV communications can be modeled as double-scattered (DS), double-shadowed (DS) fading channel. Namely, DS-DS can be modeled as the product of two Nakagami-m random variables (denoted as X_{N1} and X_{N3}) and two inverse Gamma random variables (denoted as X_{I2} and X_{I4}), given by [4, Eq. (3)]:

$$X_{out} = X_{N1} X_{I2} X_{N3} X_{I4} = \underbrace{X_{N1} \frac{1}{X_{N2}^2}}_{Y_1} \underbrace{X_{N3} \frac{1}{X_{N4}^2}}_{Y_2} \quad (1)$$

where inverse Gamma random variables can be expressed as squared inverse Nakagami-m random variables [16, Eq. (2.55)]. Namely, $X_{I2} = \frac{1}{X_{N2}^2}$ and $X_{I4} = \frac{1}{X_{N4}^2}$. Nakagami-m PDFs are, respectively [16, Eq. (2.52)]:

$$p_{X_{N,i}}(x_{N,i}) = \frac{2(m_i/\Omega_i)^{m_i}}{\Gamma(m_i)} (x_{N,i})^{2m_i-1} e^{-\frac{m_i}{\Omega_i}(x_{N,i})^2}, i = 1, 4; \quad (2)$$

The PDF of the product of Nakagami-m and inverse Gamma random variables, denoted as Y_1 can be expressed as:

$$p_{Y_1}(y_1) = \int_0^\infty \left| \frac{dx_{N1}}{dy_1} \right| p_{X_{N1}}(y_1 x_{N1}^2) p_{X_{N2}}(x_{N2}) dx_{N2} \quad (3)$$

where $\left| \frac{dx_{N1}}{dy_1} \right| = x_{N2}^2$. After substitution (2) in (3), PDF of $p_{Y_1}(y_1)$ is:

$$p_{Y_1}(y_1) = \frac{4m_1^{m_1} m_2^{m_2}}{\Omega_1^{m_1} \Omega_2^{m_2} \Gamma(m_1) \Gamma(m_2)} y_1^{2m_1-1} \times \int_0^\infty x_{N2}^{4m_1+2m_2-1} e^{-\frac{m_1}{\Omega_1} y_1^2 x_{N2}^4 - \frac{m_2}{\Omega_2} x_{N2}^2} dx_{N2} \quad (4)$$

Similarly, using the same mathematical approach PDF of y_2 where $Y_2 = Y_1 X_{N3}$ is:

$$p_{Y_2}(y_2) = \frac{8m_1^{m_1} m_2^{m_2} m_3^{m_3}}{\Omega_1^{m_1} \Omega_2^{m_2} \Omega_3^{m_3} \Gamma(m_1) \Gamma(m_2) \Gamma(m_3)} y_2^{2m_1-1} \times \int_0^\infty dx_{N2} \int_0^\infty x_{N2}^{4m_1+2m_2-1} x_{N3}^{2m_3-2m_1-1} \times e^{-\frac{m_1}{\Omega_1} \frac{y_2^2 x_{N2}^4}{x_{N3}^2} - \frac{m_2}{\Omega_2} x_{N2}^2 - \frac{m_3}{\Omega_3} x_{N3}^2} dx_{N3} \quad (5)$$

The PDF of the product of DN and DIG random variables, denoted as $p_{X_{out}}(x_{out})$, where $X_{out} = Y_2 \frac{1}{X_{N4}^2}$ can be expressed as:

$$p_{X_{out}}(x_{out}) = \int_0^\infty \left| \frac{dy_2}{dx_{out}} \right| p_{Y_2}(x_{out} x_{N4}^2) p_{X_{N4}}(N_4) dx_{N4} \quad (6)$$

where $\left| \frac{dy_2}{dx_{out}} \right| = x_{N4}^2$ and p_{Y_2} is already provided in (5).

The PDF of $p_{X_{out}}(x_{out})$ is:

$$p_{X_{out}}(x_{out}) = \frac{16(\frac{m_1}{\Omega_1})^{m_1} (\frac{m_2}{\Omega_2})^{m_2} (\frac{m_3}{\Omega_3})^{m_3} (\frac{m_4}{\Omega_4})^{m_4}}{\Gamma(m_1) \Gamma(m_2) \Gamma(m_3) \Gamma(m_4)} x_{out}^{2m_1-1} \times \int_0^\infty dx_{N2} \int_0^\infty dx_{N3} \int_0^\infty x_{N2}^{4m_1+2m_2-1} x_{N3}^{2m_3-2m_1-1} \times x_{N4}^{2m_4+4m_1-1} e^{-\frac{m_1}{\Omega_1} \frac{x_{out}^2 x_{N2}^4 x_{N4}^4}{x_{N3}^2} - \frac{m_2}{\Omega_2} x_{N2}^2 - \frac{m_3}{\Omega_3} x_{N3}^2 - \frac{m_4}{\Omega_4} x_{N4}^2} dx_{N4} \quad (7)$$

The CDF of x_{out} is expressed using [17, (3.381.1)], [17, (8.352.1)] and [17, (3.471.9)], respectively for the case where m_1 is integer:

$$F_{X_{out}}(x_{out}) = \int_0^{x_{out}} p_{X_{out}}(t) dt \times \frac{8(\frac{m_2}{\Omega_2})^{m_2} (\frac{m_3}{\Omega_3})^{m_3} (\frac{m_4}{\Omega_4})^{m_4}}{\Gamma(m_1) \Gamma(m_2) \Gamma(m_3) \Gamma(m_4)} (m_1 - 1)! \times \left(\frac{\Omega_2^{m_2} \Gamma(m_2)}{2m_2^{m_2}} \frac{\Omega_3^{m_3} \Gamma(m_3)}{2m_3^{m_3}} \frac{\Omega_4^{m_4} \Gamma(m_4)}{2m_4^{m_4}} - \sum_{k=0}^{m_1-1} \frac{(m_1 x_{out}^2)^k}{k!} E_1 \right) \quad (8)$$

where E_1 is 3-folded integral expressed as:

$$E_1 = \int_0^\infty dx_{N2} \int_0^\infty dx_{N3} \int_0^\infty x_{N2}^{2m_2+4k-1} x_{N3}^{2m_3-2k-1} \times x_{N4}^{2m_4+4k-1} e^{-\frac{m_1}{\Omega_1} \frac{x_{out}^2 x_{N2}^4 x_{N4}^4}{x_{N3}^2} - \frac{m_2}{\Omega_2} x_{N2}^2 - \frac{m_3}{\Omega_3} x_{N3}^2 - \frac{m_4}{\Omega_4} x_{N4}^2} dx_{N4} \quad (9)$$

The expression E_1 can be solved using Laplace integration (LI) approximation for three folded integrals [18]-[20]. The closed form approximation of $F_{X_{out}}(x_{out})$ can be calculated by applying [19, Eq. (I.3)]:

$$\begin{aligned} & \int_0^\infty dx_{N2} \int_0^\infty dx_{N3} \int_0^\infty f_1(x_{N2}, x_{N3}, x_{N4}) \\ & \times e^{-\gamma f_2(x_{N2}, x_{N3}, x_{N4})} dx_{N4} \\ & \approx \left(\frac{2\pi}{\gamma} \right)^{\frac{3}{2}} \frac{f_1(x_{N20}, x_{N30}, x_{N40})}{\sqrt{\det G}} e^{-\gamma f_2(x_{N20}, x_{N30}, x_{N40})} \end{aligned} \quad (10)$$

where x_{N20} , x_{N30} , x_{N40} and matrix G can be obtained from the following mathematical expressions, respectively,

$$\begin{aligned} \frac{\partial f_2(x_{N20}, x_{N30}, x_{N40})}{\partial x_{N20}} &= 0, \quad \frac{\partial f_2(x_{N20}, x_{N30}, x_{N40})}{\partial x_{N30}} = 0, \\ \frac{\partial f_2(x_{N20}, x_{N30}, x_{N40})}{\partial x_{N40}} &= 0 \end{aligned} \quad (11)$$

$$G = \begin{bmatrix} \frac{\partial^2 f_2}{\partial x_{N20}^2} & \frac{\partial^2 f_2}{\partial x_{N20} \partial x_{N30}} & \frac{\partial^2 f_2}{\partial x_{N20} \partial x_{N40}} \\ \frac{\partial^2 f_2}{\partial x_{N30} \partial x_{N20}} & \frac{\partial^2 f_2}{\partial x_{N30}^2} & \frac{\partial^2 f_2}{\partial x_{N30} \partial x_{N40}} \\ \frac{\partial^2 f_2}{\partial x_{N40} \partial x_{N20}} & \frac{\partial^2 f_2}{\partial x_{N40} \partial x_{N30}} & \frac{\partial^2 f_2}{\partial x_{N40}^2} \end{bmatrix} \quad (12)$$

The E_1 in (9) can be calculated by exponential LI for the following set of functions: $\gamma=1$, $f_1 = 1$,

$$\begin{aligned} f_2 = & \frac{m_1}{\Omega_1} \frac{x_{out}^2 x_{N2}^4 x_{N4}^4}{N_3^2} + \frac{m_2}{\Omega_2} x_{N2}^2 + \frac{m_3}{\Omega_3} x_{N3}^2 + \frac{m_4}{\Omega_4} x_{N4}^2 \\ & - (2m_2 + 4k - 1) \ln x_{N2} - (2m_3 - 2k - 1) \ln x_{N3} \\ & - (2m_4 + 4k - 1) \ln x_{N4} \end{aligned} \quad (13)$$

The LCR for a given threshold x_{TH} , denoted as $Lcr_X(x_{TH})$ is given by:

$$Lcr_X(x_{TH}) = \int_0^\infty \dot{x}_{out} p_{X_{out} \dot{X}_{out}}(x_{TH} \dot{x}_{out}) d\dot{x}_{out} \quad (14)$$

where \dot{x}_{out} is the first derivative of x_{out} . The $p_{X_{out} \dot{X}_{out}}(x_{out} \dot{x}_{out})$ can be derived from the joint PDF of independent RPs, x_{out} , \dot{x}_{out} , x_{N2} , x_{N3} and x_{N4} :

$$\begin{aligned} p_{X_{out} \dot{X}_{out}}(x_{out} \dot{x}_{out}) = & \int_0^\infty dx_{N2} \int_0^\infty dx_{N3} \\ & \times \int_0^\infty p_{X_{out} \dot{X}_{out} X_{N2} X_{N3} X_{N4}}(x_{out} \dot{x}_{out} x_{N2} x_{N3} x_{N4}) dx_{N4} \end{aligned} \quad (15)$$

where $p_{X_{out} \dot{X}_{out} X_{N2} X_{N3} X_{N4}}(x_{out} \dot{x}_{out} x_{N2} x_{N3} x_{N4})$ can be transformed as:

$$\begin{aligned} & p_{X_{out} \dot{X}_{out} X_{N2} X_{N3} X_{N4}}(x_{out} \dot{x}_{out} x_{N2} x_{N3} x_{N4}) \\ & = p_{\dot{X}_{out} | X_{out} X_{N2} X_{N3} X_{N4}}(\dot{x}_{out} | x_{out} x_{N2} x_{N3} x_{N4}) \\ & \times p_{X_{out} | X_{N2} X_{N3} X_{N4}}(x_{out} | x_{N2} x_{N3} x_{N4}) \\ & \times p_{X_{N2}}(x_{N2}) p_{X_{N3}}(x_{N3}) p_{X_{N4}}(x_{N4}) \end{aligned} \quad (16)$$

where,

$$p_{X_{out} | X_{N2} X_{N3} X_{N4}} = \left| \frac{dx_{N1}}{dx_{out}} \right| p_{x_{N1}} \left(\frac{x_{out} x_{N2}^2 x_{N4}^2}{x_{N3}} \right) \quad (17)$$

After substitutions, (17) in (16), (16) in (15) and (15) in (14), respectively, the $Lcr_X(x_{TH})$ becomes:

$$\begin{aligned} Lcr_X(x_{TH}) = & \int_0^\infty dx_{N2} \int_0^\infty \left| \frac{dx_{N1}}{dx_{out}} \right| p_{x_{N1}} \left(\frac{x_{TH} x_{N2}^2 x_{N4}^2}{x_{N3}} \right) \\ & \times p_{X_{N2}}(x_{N2}) p_{X_{N3}}(x_{N3}) p_{X_{N4}}(x_{N4}) dx_{N3} \\ & \times \int_0^\infty \dot{x}_{out} p_{\dot{X}_{out} | X_{out} X_{N2} X_{N3} X_{N4}}(\dot{x}_{out} | x_{out} x_{N2} x_{N3} x_{N4}) d\dot{x}_{out} \end{aligned} \quad (18)$$

where,

$$\int_0^\infty \dot{x}_{out} p_{\dot{X}_{out} | X_{out} X_{N2} X_{N3} X_{N4}} = \frac{1}{\sqrt{2\pi}} \sigma_{\dot{x}_{out}} \quad (19)$$

The first derivative of the x_{out} can be expressed as:

$$\begin{aligned} \dot{x}_{out} = & \frac{x_{N3} \dot{x}_{N1}}{x_{N2}^2 x_{N4}^2} - 2 \frac{x_{N1}}{x_{N2}^3} \frac{x_{N3} \dot{x}_{N2}}{x_{N4}^2} \\ & + \frac{x_{N1} \dot{x}_{N3}}{x_{N2}^2 x_{N4}^2} - 2 \frac{x_{N1}}{x_{N2}^2} \frac{x_{N3} \dot{x}_{N4}}{x_{N4}^3} \end{aligned} \quad (20)$$

where $\dot{x}_{N1}, \dot{x}_{N2}, \dot{x}_{N3}$ and \dot{x}_{N4} are the first derivatives of x_{N1}, x_{N2}, x_{N3} and x_{N4} , respectively. Since the linear transformation of zero mean Gaussian RVs is a zero mean Gaussian RV, the variance of \dot{x}_{out} is also a zero mean Gaussian RV and $\sigma_{\dot{x}_{out}}^2$ can be expressed through the variances of $\dot{x}_{N1}, \dot{x}_{N2}, \dot{x}_{N3}$ and \dot{x}_{N4} expressed as $\sigma_{\dot{x}_{N1}}^2, \sigma_{\dot{x}_{N2}}^2, \sigma_{\dot{x}_{N3}}^2$ and $\sigma_{\dot{x}_{N4}}^2$, respectively:

$$\begin{aligned} \sigma_{\dot{x}_{out}}^2 = & \frac{x_{N3}^2}{x_{N2}^4 x_{N4}^4} \sigma_{\dot{x}_{N1}}^2 \left(1 + \frac{4x_{out}^2 x_{N2}^2 x_{N4}^4}{x_{N3}^2} \sigma_{\dot{x}_{N2}}^2 / \sigma_{\dot{x}_{N1}}^2 \right. \\ & \left. + \frac{x_{out}^2 x_{N2}^4 x_{N4}^4}{N_3^4} \sigma_{\dot{x}_{N3}}^2 / \sigma_{\dot{x}_{N1}}^2 + \frac{4x_{out}^2 x_{N2}^4 x_{N4}^2}{x_{N3}^2} \sigma_{\dot{x}_{N4}}^2 / \sigma_{\dot{x}_{N1}}^2 \right) \end{aligned} \quad (21)$$

Finally, the $Lcr_X(x_{TH})$ can be expressed as:

$$Lcr_X(x_{TH}) = \frac{16 \sigma_{\dot{x}_{N1}}^2 \left(\frac{m_1}{\Omega_1} \right)^{m_1} \left(\frac{m_2}{\Omega_2} \right)^{m_2} \left(\frac{m_3}{\Omega_3} \right)^{m_3} \left(\frac{m_4}{\Omega_4} \right)^{m_4} x_{TH}^{2m_1-1}}{\sqrt{2\pi} \Gamma(m_1) \Gamma(m_2) \Gamma(m_3) \Gamma(m_4)} E_2 \quad (22)$$

where, E_2 is a 3-folded integral given by:

$$\begin{aligned} E_2 = & \int_0^\infty dx_{N2} \int_0^\infty dx_{N3} \int_0^\infty dx_{N4} \\ & \times \left(1 + \frac{4x_{TH}^2 x_{N2}^2 x_{N4}^4}{x_{N3}^2} \sigma_{\dot{x}_{N2}}^2 / \sigma_{\dot{x}_{N1}}^2 + \frac{x_{TH}^2 x_{N2}^4 x_{N4}^4}{N_3^4} \sigma_{\dot{x}_{N3}}^2 / \sigma_{\dot{x}_{N1}}^2 \right. \\ & \left. + \frac{4x_{TH}^2 x_{N2}^2 x_{N4}^4}{x_{N3}^2} \sigma_{\dot{x}_{N4}}^2 / \sigma_{\dot{x}_{N1}}^2 \right)^{\frac{1}{2}} x_{N2}^{2m_2+4m_1-3} x_{N3}^{2m_3-2m_1} \\ & \times x_{N4}^{2m_4+4m_1-3} e^{-\frac{m_1}{\Omega_1} \frac{x_{TH}^2 x_{N2}^4 x_{N4}^4}{x_{N3}^2} - \frac{m_2}{\Omega_2} x_{N2}^2 - \frac{m_3}{\Omega_3} x_{N3}^4 - \frac{m_4}{\Omega_4} x_{N4}^2} dx_{N4} \end{aligned} \quad (23)$$

The integral E_2 can be solved by LI, already given by (10), (11) and (12) for the following γ , $f_1(x_{N2}, x_{N3}, x_{N4})$ and $f_2(x_{N2}, x_{N3}, x_{N4})$, respectively: $\gamma=1$,

$$\begin{aligned} f_1 = & \left(1 + \frac{4x_{TH}^2 x_{N2}^2 x_{N4}^4}{x_{N3}^2} \sigma_{\dot{x}_{N2}}^2 / \sigma_{\dot{x}_{N1}}^2 \right. \\ & \left. + \frac{x_{TH}^2 x_{N2}^4 x_{N4}^4}{x_{N3}^4} \sigma_{\dot{x}_{N3}}^2 / \sigma_{\dot{x}_{N1}}^2 + \frac{4x_{TH}^2 x_{N2}^4 x_{N4}^2}{x_{N3}^2} \sigma_{\dot{x}_{N4}}^2 / \sigma_{\dot{x}_{N1}}^2 \right)^{\frac{1}{2}} \end{aligned} \quad (24)$$

$$\begin{aligned}
f_2 = & \frac{m_1}{\Omega_1} \frac{x_{TH}^2 x_{N2}^4 x_{N4}^4}{x_{N3}^2} + \frac{m_2}{\Omega_2} x_{N2}^2 + \frac{m_3}{\Omega_3} x_{N3}^4 + \frac{m_4}{\Omega_4} x_{N4}^2 \\
& - (2m_2 + 4m_1 - 3) \ln x_{N2} - (2m_3 - 2m_1) \ln x_{N3} \\
& - (2m_4 + 4m_1 - 3) \ln x_{N4}
\end{aligned} \quad (25)$$

The average fade duration (AFD) for a given threshold x_{TH} , denoted as $Afd_X(x_{TH})$ can be evaluated as:

$$Afd_X(x_{TH}) = \frac{F_X(x_{TH})}{Lcr_X(x_{TH})} \quad (26)$$

The system model from UAV-to-ground communications is extended to include selection of UAV with the highest signal envelope level from among N -UAVs over N i.n.i.d ground-to-UAV links.

The CDF for extended UAV channel model over DS-DS fading, denoted as $F_X^{(S)}(x)$ can be expressed as:

$$F_X^{(S)}(x) = F_X(x)^N \quad (27)$$

LCR with UAV selection over DS-DS fading can be obtained as:

$$Lcr_X^{(S)}(x_{th}) = NLcr_X(x_{TH})F_X(x_{TH})^{N-1} \quad (28)$$

Finally, the $Afd_X^{(S)}(x_{th})$ for DS-DS channel model with UAV selection is:

$$Afd_X^{(S)}(x_{th}) = \frac{F_X(x_{TH})}{NLcr_X(x_{TH})} \quad (29)$$

III. NUMERICAL RESULTS

The SO statistics of UAV-to-ground communications over DS-DS channel fading model in terms of various fading DS-DS severities are efficiently evaluated and presented in numerical results. Moreover, the SO statistics of the extended model with UAV selection is then numerically evaluated and investigated in terms of different system model parameters. The presented results show that exact analytical expression (integral form expression) for $Lcr_X(x_{TH})$ fits well with the approximation (closed form expressions approximated by LI). Moreover, the exact analytical expression (integral form expression) for $F_X(x)$ is approximated by exponential LI. The presented results for $Afd_X(x_{TH})$ (ratio of $Lcr_X(x_{TH})$ and $F_X(x_{TH})$) between exact form solution and approximation fits well only for higher x_{TH} values.

The DS-DS fading channel is modeled as the product of DN and DIG, where results are presented for various DS-DS multipath severity parameters (m_1, m_3) and various values of DS-DS shadowing severity parameters (m_2, m_4). The variances in (21) are expressed as $\sigma_{x_{Ni}}^2 = \pi^2 f_{mi}^2 \frac{\Omega_i}{m_i}$, $i = 1, 4$ where the maximum Doppler frequencies are assumed to be the same [19, Eq. (43)], $f_m = f_{mi} = \sqrt{f_{m_{Tx}}^2 + f_{m_{Rx}}^2}$.

Fig. 1 provides the behavior of $Lcr_X(x_{TH})$ normalized by f_m . It can be seen that by increasing all DS-DS severity parameters, $Lcr_X(x_{TH})$ decreases in the whole observable x_{TH} dB regime, which in turn can provide improvement in the

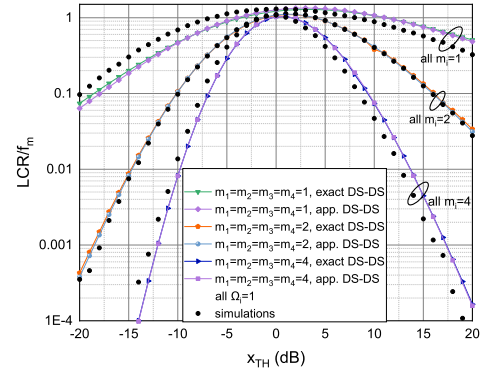


Fig. 1. $Lcr_X(x_{TH})$ normalized by f_m versus x_{TH} under different fading severity conditions.

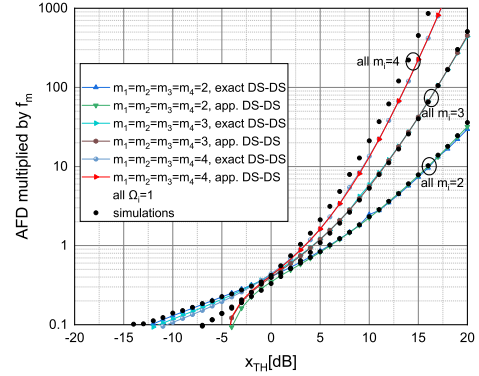


Fig. 2. $Afd_X(x_{TH})$ multiplied by f_m versus x_{TH} for DS-DS type of fading and under different fading severity conditions.

system performances. The behavior of $Afd_X(x_{TH})$ multiplied by f_m is provided in Fig. 2. The numerical results show that by increasing all DS-DS severity parameters, $Afd_X(x_{TH})$ slightly decreases in lower x_{TH} threshold dB regime while $Afd_X(x_{TH})$ increases in higher x_{TH} dB regime. Moreover, the impact of DS-DS fading severities on $Afd_X(x_{TH})$ is stronger for higher x_{TH} .

Fig. 3 provides normalized $Lcr_X^{(S)}(x_{th})$. The increasing number of UAVs causes $Lcr_X^{(S)}(x_{th})$ values to decrease for lower x_{th} and $Lcr_X^{(S)}(x_{th})$ values to increase for higher x_{th} . Moreover, it can be observed that the number of UAVs have stronger impact on $Lcr_X^{(S)}(x_{th})$ for lower dB x_{th} values. The $Afd_X^{(S)}(x_{th})$ multiplied by f_m is presented in Fig 4. It is evident that increasing number of UAVs, can improve system performances, since $Afd_X^{(S)}(x_{th})$ decreases in whole x_{th} dB regime. Similarly, it can be noticed that number of UAVs have stronger impact on $Afd_X^{(S)}(x_{th})$ for lower x_{th} .

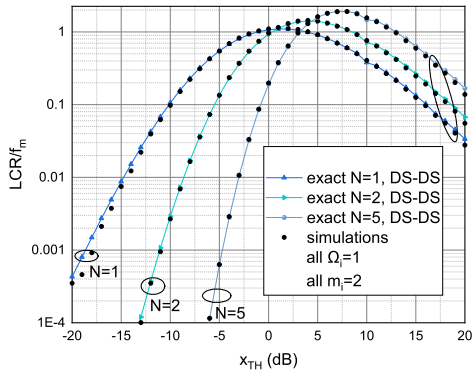


Fig. 3. $Lcr_X^{(S)}(x_{th})$ normalized by f_m with selection from among N UAVs over DS-DS type of fading.

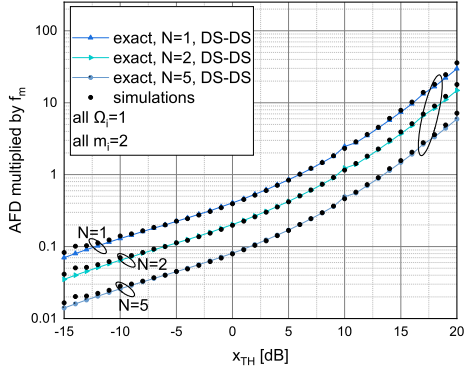


Fig. 4. $Afd_X^{(S)}(x_{th})$ multiplied by f_m with selection from among N UAVs over DS-DS type of fading.

IV. CONCLUSION

The SO statistics in urban UAV-to-ground communication systems over DS-DS fading channel is considered. The model is extended to include UAV selection with the highest signal envelope level from among N -UAVs over N i.n.i.d links. In particular, we provide mathematical expressions for the SO statistics of the product of DN and DIG RPs. The LI approximation formulas for derivation of closed form analytical expressions as well as Monte Carlo simulations for verification of obtained results are efficiently applied. The increase in DS-DS multipath and shadowing fading severity parameters can provide system performance improvement for lower dB threshold values in relation to SO statistics. Moreover, the increasing number of UAVs can further provide system performance improvements.

V. ACKNOWLEDGMENT

C. Stefanovic would like to acknowledge CONEX-Plus. The CONEX-Plus is funded by UC3M, the European Commiss-

sion through the Marie Skłodowska Curie COFUND Action (H2020-MSCA-COFUND-2017- GA 801538).

REFERENCES

- [1] A. A. Khuwaja, Y. Chen, N. Zhao, M. S. Alouini and P. Dobbins, "A survey of channel modeling for UAV communications", *IEEE Communications Surveys and Tutorials*, vol. 20, no. 4, pp. 2804–2821, 2018.
- [2] L. Zhu, D. He, K. Ghuan, B. Ai, Z. Zhong and D. Li, "Channel characterization and simulation for unmanned aerial vehicle communication", *IEEE International Symposium on Antennas and Propagation and USNC-USRI Radio Science Meeting*, pp. 2135–2136, 2019.
- [3] P. S. Bithas, V. Nikolaidis, A. G. Kanatas and G. K. Karagiannidis, "UAV-to-ground communications: channel modeling and UAV selection", *IEEE Trans. Commun.*, vol. 68, no. 8, pp. 5135 – 5144, 2020.
- [4] P. S. Bithas, V. Nikolaidis and A. G. Kanatas, "UAV-to-ground communications: a new shadowed double-scattering model with application to UAV-to-ground communications", *IEEE Wireless Communications and Networking Conference (WCNC)*, 2019.
- [5] D. Dixit, N. Kumar, S. Sharma, V. Bhatia, S. Panic and C. Stefanovic, "On the ASER Performance of UAV-Based Communication Systems for QAM Schemes," *IEEE Communications Letters*, 2021, doi:10.1109/LCOMM.2021.3058212.
- [6] L. Bai, R. Han, J. Lui, Q. Yu, J. Choi and W. Zhang, "Air-to-ground wireless links for high-speed UAVs", *IEEE Journal on Selected Areas in Communications*, 2020. DOI: 10.1109/JSAC.2020.3005471.
- [7] S. G. Sanchez, S. Mohanti, D. Jaisinghami and K. R. Chowdhury, "Millimeter-wave base stations in the Sky: An experimental study of UAV-to-ground communications", *IEEE Transactions on Mobile Computing*, 2020. DOI: 10.1109/TMC.2020.3013575.
- [8] M. T. Dabiri, S. M. S. Sadough and M. A. Khalighi, "Channel modeling and parameter optimization for hovering UAV-based free-space optical links", *IEEE Journal on Selected Areas in Communications*, vol. 36, no. 9, pp. 2104–2113, 2018.
- [9] S. Panic, T. D. P. Perera, D. N. K. Jayakody, C. Stefanovic and B. Prelincevic, "UAV-assisted wireless powered sensor network over Rician shadowed fading channels", *IEEE International Conference on Microwaves, Antennas, Communications and Electronic Systems*, 2019.
- [10] S. K. Yoo, S. L. Cotton, P. C. Sofotasios, S. Muhaidat and G. K. Karagiannidis, "Average fade duration for amplify-and-forward relay networks in fading channels", *IEEE Wireless Communications Letters*, vol. 9, no. 3, pp. 281–284, 2020.
- [11] Q. Zhu, N. Cheng, X. Chen, W. Zhong, B. Hua and Y. Wang, "Envelope level crossing rate and average fade duration of a generic 3D non-stationary UAV channel model", *IEEE Access*, vol. 8, pp. 143134–143143, 2020.
- [12] Y. Wang, N. Cheng, X. Chen, W. Fan, Q. Zhu and W. Zhong, "Second order statistics of simulation models for UAV-MIMO Ricean fading channels", *IEEE International Conference on Communications (ICC)* , 2019.
- [13] F. Jameel, M. A. A. Haider and A. A. Butt, "Second order fading statistics of UAV networks", *IEEE Fifth International Conference on Aerospace Science Engineering (ICASE)*, 2017.
- [14] M. Simunek, F. P. Fontan and P. Pechac, "The UAV low elevation propagation channel in urban areas: Statistical analysis and time-series generator", *IEEE Trans. Antennas Propag.*, vol. 61, no. 7, pp. 3850–3858, 2013.
- [15] M. Simunek, F. P. Fontan, P. Pechac and F. J. Otero, "Space diversity gain in urban area low elevation links for surveillance applications", *IEEE Trans. Antennas Propag.*, vol. 61, no. 12, pp. 6255–6260, 2013.
- [16] L. G. Stuber, *Principles of mobile communication*, Norwell, Mass, USA: Kluwer Academic, 1996.
- [17] I. S. Gradshteyn and I. M. Ryzhik, *Table of Integrals, Series, and Products*, New York: Academic, 2000.
- [18] Z. N. Zlatanov, Z. Hadzi-Velkov and G. K. Karagiannidis, "Level crossing rate and average fade duration of the double Nakagami-m random process and application in MIMO keyhole fading channels", *IEEE Communications Letters*, vol. 12, no. 11, pp. 822–824, 2008.
- [19] Z. Hadzi-Velkov, Z. N. Zlatanov and G. K. Karagiannidis, "On the second order statistics of the multihop Rayleigh fading channel", *IEEE Transactions on Communications*, vol. 57, no. 6, pp. 1815 – 1823, 2009.
- [20] N. Hajri, R. Khedhiri and N. Youssef, "On selection combining diversity in dual-hop relaying systems over double Rice channels: fade statistics and performance analysis", *IEEE Access*, vol. 8, pp. 72188–72203, 2020.